

Electronic Supplementary Information

Polylysine-Grafted Au₁₄₄ Nanoclusters: Birth and Growth of a Healthy Surface-Plasmon-Resonance-like Band

Ivan Guryanov,^{a,*} Federico Polo,^b Evgeniy V. Ubyvovk,^c Evgenia Korzhikova-Vlakh,^a Tatiana Tennikova,^a Armin T. Rad,^d Mu-Ping Nieh,^{e,f} and Flavio Maran^{b,g,*}

^aInstitute of Chemistry, St. Petersburg State University, 26 Universitetskij Pr., 198504 Petrodvorets, St. Petersburg, Russia

^bDepartment of Chemistry, University of Padova, Via Marzolo 1, 35131 Padova, Italy

^cDepartment of Physics, St. Petersburg State University, 3 Ulyanovskaya, 198504 Petrodvorets, St. Petersburg, Russia

^dDepartment of Biomedical Engineering, University of Connecticut, 260 Glenbrook Road, Storrs, Connecticut 06269, USA

^ePolymer Program, Institute of Materials Science, University of Connecticut, 97 N. Eagleville Rd, Storrs, Connecticut 06269, USA

^fDepartment of Chemical & Biomolecular Engineering, University of Connecticut, 191 Auditorium Rd, Storrs, Connecticut 06269, USA

^gDepartment of Chemistry, University of Connecticut, 55 N. Eagleville Rd, Storrs, Connecticut 06269, USA

Table of Contents

1. Materials and Methods
2. Synthesis
3. SAXS Analysis
4. Supplementary Figures
5. References

1. Materials and Methods

The following solvents, salts, and reagents were commercially available and used as received. Solvents: ethanol, methanol, toluene, dichloromethane, diethyl ether, petroleum ether, ethyl acetate, acetonitrile, dimethylformamide (Sigma-Aldrich). Salts: potassium bisulfate, sodium bicarbonate, anhydrous sodium sulfate (Carlo Erba);. Reagents: 99.9+% hydrogen tetrachloroauratetrihydrate, tetra-*n*-octylammonium bromide, sodium borohydride, triisopropylsilane, trifluoroacetic acid, S-

trityl-3-mercaptopropionic acid, ethylenediamine, triphosgene, α -pinene, triethylamine, 10% palladium on activated carbon, iodine (Sigma-Aldrich); 1-(3-dimethyl-aminopropyl)-3-ethylcarbodiimide hydrochloride, 1-hydroxy-7-aza-1,2,3-benzotriazole (GL Biochem), *N*-fluorenylmethyloxycarbonylsuccinimide, *N,N*-diisopropylethylamine, α -benzyloxycarbonyl lysine, piperidine (Iris Biotech). Flash chromatography was performed using silica gel 60 M (0.04 - 0.063 mm, Macherey-Nagel) as stationary phase. Chloroform-*d* (99.8%, Aldrich), acetonitrile-*d*₃ (99.8%, Aldrich), methanol-*d*₄ (99.8%, Aldrich), dimethyl sulfoxide-*d*₆ (99.9%, Aldrich) and water-*d*₂ (99.9%, Aldrich) were used as solvents for NMR spectroscopy.

Analytical thin-layer chromatography (TLC) was carried out by using Macherey-Nagel TLC-cards (0.2 mm silica gel supported on plastic sheets). The spots were visualized first with UV light ($\lambda = 254$ nm) and then after exposure to iodine vapor and KMnO₄ aqueous solution. ¹H NMR spectra were recorded by using a Bruker model AC 200 and Avance-400 DRX spectrometers, operating at 200 and 400 MHz, respectively. Chemical shifts (δ) are given as parts per million (ppm) downfield from tetramethylsilane, which was added as the internal standard. Splitting patterns are abbreviated as follows: (s) singlet, (d) doublet, (t) triplet, (q) quartet, (m) multiplet. The proton assignments were carried out by standard chemical shift correlations. When possible, the monolayer composition was determined by decomposing the MPC with iodine. To this aim a crystal of iodine was added to the solution of AuMPC in NMR tube and the NMR spectrum was registered after formation of a black precipitate. The solution of the liberated ligands was analyzed through a comparison between the integrals of conveniently separated peaks, as illustrated in Figures S3-S5.

2. Synthesis

Au₁₄₄(SCH₂CH₂Ph)₆₀ nanocluster were prepared and carefully purified as already described.^{S1,S2}

TrtS-CH₂CH₂CO-NHCH₂CH₂NH₂. TrtS-CH₂CH₂COOH (1 g, 2.87 mmol) and HOAt (0.47 g, 3.44 mmol) were dissolved in 20 ml of anhydrous dichloromethane and EDC·HCl (0.66 g, 3.44 mmol) was added. The reaction mixture was stirred for 2 h, and then a solution of diaminoethylene (1.9 ml, 28.70 mmol) in 50 ml of dichloromethane was added dropwise during 1 h. After 2 days the solvent was evaporated and the crude product was purified by flash chromatography using as eluent dichloromethane, and then the mixtures dichloromethane/ methanol (v/v 95/5, 90/10, 80/20) and recrystallized from the mixture of 5 ml of methanol and 20 ml of ethyl acetate with dropwise addition of petroleum ether. Yield: 0.75 g (67%). IR (KBr): 3420, 3262, 3082, 3055, 3022, 2937, 2900, 1654, 1560, 1483, 1447 cm⁻¹; ¹H NMR (200 MHz, CD₃OD): δ 7.15 – 7.47 (m, 16H; 15 H, Trt, 1H, NH), 3.42 (t, 2H, CH₂, *J* = 6 Hz), 3.03 (t, 2H, CH₂, *J* = 6 Hz), 2.47 (t, 2H, CH₂, *J* = 6 Hz), 2.27 (t, 2H, CH₂, *J* = 6 Hz).

TrtS-CH₂CH₂CO-NHCH₂CH₂NHFmoc. TrtS-CH₂CH₂CO-NHCH₂CH₂NH₂ (1.3 g, 3.33 mmol) was dissolved in 20 ml of acetonitrile, a solution of Fmoc-OSu (1.12 g, 3.33 mmol) in 20 ml of acetonitrile and diisopropylethylamine (0.56 ml, 3.33 mmol) were added. The reaction mixture was stirred for 24 h and concentrated to 20 ml. The white precipitate was filtered, washed with 5 ml of acetonitrile cooled to 0°C and dried. The organic solutions were collected, the solvent was evaporated and the product was recrystallized from acetonitrile. The total yield: 1.25 g (62%). IR (KBr): 3415, 3304, 3060, 2941, 1696, 1652, 1548, 1445, 1267 cm⁻¹; ¹H NMR (200 MHz, CDCl₃): δ 7.55 (d, 2H, CH Fmoc, *J* = 8 Hz), 7.51 (d, 2H, CH Fmoc, *J* = 8 Hz), 7.20 – 7.50 (m, 19H; 15 H, Trt, 4H, Fmoc), 5.75 (s, 1H, NH), 5.20 (s, 1H, NH), 4.30 (d, 2H, CH₂Fmoc, *J* = 6 Hz), 4.15 (t, 1H, CH Fmoc, *J* = 6 Hz), 3.26 (s, 4H, 2CH₂), 2.50 (t, 2H, CH₂, *J* = 6 Hz), 2.10 (t, 2H, CH₂, *J* = 6 Hz).

HS-CH₂CH₂CO-NHCH₂CH₂NH₂·TFA (Ligand 1). TrtS-CH₂CH₂CO-NHCH₂CH₂NH₂ (0.21 g, 0.54 mmol) and 0.5 ml of TIS (2.44 mmol) were dissolved in 15 ml of dichloromethane. 2 ml of TFA were added dropwise and the reaction

mixture was stirred for 1 h. The solvent was evaporated and 20 ml of diethyl ether were added to the white solid. The product was filtered, washed 6×20 ml of diethyl ether and dried. Yield: 135 mg (95%). ¹H NMR (200 MHz, ACN-*d*₃): δ 7.84 (s, 3H, NH₃⁺), 7.69 (s, 1H, NH), 3.47 (q, 2H, CH₂, *J* = 4 Hz), 3.09 (t, 2H, CH₂, *J* = 6 Hz), 2.72 (q, 2H, CH₂, *J* = 8 Hz), 2.49 (t, 2H, CH₂, *J* = 6 Hz), 1.79 (t, 1H, SH, *J* = 8 Hz).

HS-CH₂CH₂CO-NHCH₂CH₂NHFmoc (Ligand 2). TrtS-CH₂CH₂CO-NHCH₂CH₂NHFmoc (0.3 g, 0.49 mmol) and 0.5 ml of TIS (2.44 mmol) were dissolved in 8 ml of dichloromethane. 1.5 ml of TFA were added dropwise and the reaction mixture was stirred for 1 h. The solvent was evaporated and 20 ml of diethyl ether were added to the white solid. The product was filtered, washed 6×20 ml of diethyl ether and dried. Yield: 170 mg (92%). IR (KBr): 3312, 3068, 2949, 1682, 1645, 1549, 1445, 1260 cm⁻¹; ¹H NMR (200 MHz, CDCl₃): δ 7.77 (d, 2H, CH Fmoc, *J* = 8 Hz), 7.58 (d, 2H, CH Fmoc, *J* = 8 Hz), 7.25 – 7.48 (m, 4H, Fmoc), 6.08 (s, 1H, NH), 5.19 (s, 1H, NH), 4.43 (d, 2H, CH₂Fmoc, *J* = 6 Hz), 4.21 (t, 1H, CH Fmoc, *J* = 6 Hz), 3.37 (s, 4H, 2CH₂), 2.78 (q, 2H, CH₂, *J* = 8 Hz), 2.46 (t, 2H, CH₂, *J* = 6 Hz), 1.57 (t, 1H, SH, *J* = 8 Hz).

Z-Lys(Fmoc)-OH. Z-Lys-OH (5 g, 17.8 mmol) was suspended in 150 ml of water, and 7.75 ml (44.5 mmol) of triethylamine were added to get a clear solution. A solution of 7.2 g (21.4 mmol) of Fmoc-OSu in 100 ml of acetonitrile was added portionwise during 6 h. Then the organic solvent was evaporated, the water solution was washed with diethyl ether (3×100 ml) and pH was adjusted to 2 with 1M H₂SO₄. The product was extracted with ethyl acetate (3×100 ml), the solvent was dried over Na₂SO₄ and evaporated. The product was obtained as a slightly yellow oil. Yield: 7.7 g, 86%. IR (KBr): 3356, 3320, 3068, 2942, 1742, 1690, 1638, 1541, 1452, 1267 cm⁻¹; ¹H NMR (200 MHz, CDCl₃): δ 7.75 (d, 2H, CH Fmoc, *J* = 8 Hz), 7.56 (d, 2H, CH Fmoc, *J* = 8 Hz), 7.25 – 7.48 (m, 9H; 4H, Fmoc, 5H Z), 5.64 (t, 1H, NH, *J* = 8 Hz), 5.09 (s, 2H, CH₂), 4.91 (d, 1H, NH), 4.43 (m, 3H; 2H, CH₂Fmoc; 1H CH), 4.21 (t, 1H, CH Fmoc, *J* = 6 Hz), 3.01 – 3.26 (m, 2H, CH₂), 1.65 – 1.85 (m, 2H, CH₂), 1.15 – 1.60 (m, 4H, CH₂).

H-Lys(Fmoc)-OH. Z-Lys(Fmoc)-OH (2.8 g, 5.57 mmol) was dissolved in 150 ml of methanol and 0.5 g of Pd/C were added. The hydrogenation was continued till the complete disappearance of starting material and the formation of the white precipitate. The reaction mixture was concentrated to 50 ml and 50 ml of water were added to dissolve the product. Then the catalyst was filtered off, the organic solvent was evaporated and H-Lys(Fmoc)-OH was recrystallized from water. The white crystals were filtered and dried *in vacuo* over P₂O₅. Yield 1.5 g (75%). IR (KBr): 3386, 2942, 1697, 1623, 1586, 1534, 1445, 1393, 1252 cm⁻¹; ¹H NMR (200 MHz, methanol-*d*₄): δ 7.79 (d, 2H, CH Fmoc, *J* = 8 Hz), 7.64 (d, 2H, CH Fmoc, *J* = 8 Hz), 7.27 – 7.42 (m, 6H; 4H, Fmoc), 4.35 (d, 1H; CH Fmoc, *J* = 8 Hz), 4.20 (t, 2H, CH₂Fmoc, *J* = 6 Hz), 3.50 (m, 1H, CH, *J* = 8 Hz), 3.12 (t, 2H, CH₂, *J* = 8 Hz), 2.00 – 1.60 (m, 2H, CH₂), 1.60 – 1.26 (m, 4H, CH₂).

NCA of H-Lys(Fmoc)-OH was prepared accordingly to procedure described previously.^{S3}

Ligand place-exchange reaction. 150 mg (0.004 mmol) of Au₁₄₄(SCH₂CH₂Ph)₆₀ were dissolved in 20 ml of dichloromethane, a solution of 91 mg or 137 mg (0.246 mmol, 1 eq or 0.369 mmol, 1.5 eq, respectively) of HS-CH₂CH₂CO-NHCH₂CH₂NHFmoc in 20 ml of dichloromethane was added. The reaction mixture was stirred for 24 h and the solvent was rotary evaporated. The solid residue was washed with methanol (10×10 ml), and acetonitrile (5×10 ml). Removal of free ligands and disulfides was checked by thin-layer chromatography on silica plates, using 20:1 DCM:MeOH, followed by developing with iodine. The amount of the new entered ligand was determined by decomposing the MPC with iodine and analyzing the liberated ligands as disulfides by ¹H NMR and TGA. The obtained Fmoc-protected MPC were treated for 20 min with 5 ml of 20% solution of piperidine in DMF and precipitated with 50 ml of methanol. The precipitate was washed with methanol (3×50 ml) and diethyl ether (3×50 ml) and redissolved in 30 ml of chloroform. Insoluble part was filtered off, the

organic solvent was rotary evaporated, the product was dried in *in vacuo* over P₂O₅ and characterized with UV and IR spectroscopy and TGA. Yield 97 mg (65%).

3. SAXS Analysis

The SAXS intensity, I , was corrected by transmission and empty cell scattering and circularly averaged with respect to the beam center, yielding $I(q)$ as a function of scattering vector, q . For particulate systems, $I(q)$ is proportional to the product of the volume fraction of particles, the contrast factor ($\Delta\rho^2$, square of the difference in electron scattering length densities, between the particles and medium), the form factor describing the shape of the particles [*i.e.*, $P(q)$], and the structure factor describing the interparticulate interactions [*i.e.*, $S(q)$]. Hence, $I(q)$ can be expressed as

$$I(q) \propto C_{tp} \Delta\rho^2 P(q) S(q)$$

The chemical structures of the Au nanoclusters and solvent (*i.e.*, 10% acetic acid solution) are known and, therefore, $\Delta\rho$ can be calculated accordingly. To obtain possible structures of the aggregates, suitable models for $P(q)$ and $S(q)$ are required. Mathematically, the scattering amplitude, $A(q)$ of a discrete particle can be derived by its Fourier transform from the real space to the reciprocal (scattering) space (*i.e.*, q -space). The form factor of the particle, $P(q)$, is the square, to be exact the conjugate product of $A(q)$. The Au nanocluster is formed by a spherical core surrounded by a shell of ligands and, therefore, it is reasonable to use a core-shell spherical model to fit the SAXS data. It is also known that the NPs have a reasonably uniform electron density. The shell can be approximated as a single or a double layer, depending on the density of the ligands along the radial direction. The core-single shell spherical model (shown in Figure S17) can fit the SAXS data of Au(50)-I and Au(100)-I reasonably well. However, our attempt to fit the SAXS data of Au(150)-I by using a core-single shell spherical model was not successful, presumably due to the significant difference in the electron densities of the inner and outer parts of the shell. As a result, a core-two-shell spherical model (Figure S17), where the two shells are assumed to have distinct but uniform electron densities, was used to fit the SAXS data of Au(150)-I. Eqs S1 and S2 are the mathematical forms for the core-single and core-two-shell models, respectively. Because of the low concentrations of the samples, interparticle interaction is presumably negligible, yielding $S(q) = 1$.

Core-Shell Model:

$$P(q) = \frac{9\phi}{V_{NP}} \left[\frac{V_{core} \Delta\rho_{c-s} j_1(qR_{core})}{qR_{core}} + \frac{V_{NP} \Delta\rho_{s-solv} j_1(qR_{NP})}{qR_{NP}} \right]^2 \quad (S1)$$

where ϕ , V_{NP} , V_{core} , R_{core} and R_{NP} are the volume fraction (*i.e.*, concentration), the volume of the NP, the volume of the NP core, the radius of the core, and the radius of the whole NP (*i.e.*, $R_{core} + t_{shell}$, where t_{shell} is the thickness of the shell), respectively. $\Delta\rho_{c-s}$ and $\Delta\rho_{s-solv}$ are the electron-density differences between core and shell and shell and solvent, respectively. $j_1(x) = \frac{\sin x - x \cos x}{x^2}$.

Core-two-Shell Model:

$$P(q) = \frac{9\phi}{V_{NP}} \left[\frac{V_{core} \Delta\rho_{c-s1} j_1(qR_{core})}{qR_{core}} + \frac{V_{s1} \Delta\rho_{s1-s2} j_1(qR_{shell1})}{qR_{shell1}} + \frac{V_{NP} \Delta\rho_{s2-solv} j_1(qR_{NP})}{qR_{NP}} \right]^2 \quad (S2)$$

where V_{s1} , R_{shell1} , R_{NP} , $\Delta\rho_{s1-s2}$ and $\Delta\rho_{s2-solv}$ are the volume of the inner shell (shell 1), the radius of core and shell 1 (*i.e.*, $R_{core} + t_{shell}$, as indicated in Figure S16), the electron-density differences between shell 1 and shell 2 and shell 2 and solvent, respectively. It should be noted that polydispersity of R_{core} is considered using Schulz distribution function as shown below.

$$f(R_{core}) = (z + 1)^{z+1} \left(\frac{R_{core}}{\langle R_{core} \rangle} \right)^z \frac{e^{-\frac{(z+1)R_{core}}{\langle R_{core} \rangle}}}{\langle R_{core} \rangle \Gamma(z + 1)}$$

where $\langle R_{core} \rangle$ is the average R_{core} and $z = \frac{1}{p^2} - 1$, where p is the polydispersity defined as $\frac{\sigma}{\langle R_{core} \rangle}$ with σ being the standard deviation of R_{core} . $\Gamma(x)$ is the Gamma function. The fitting programs of the two SANS models are available at the NIST center for neutron research using IGOR Pro v6.^{S4}

4. Supplementary Figures

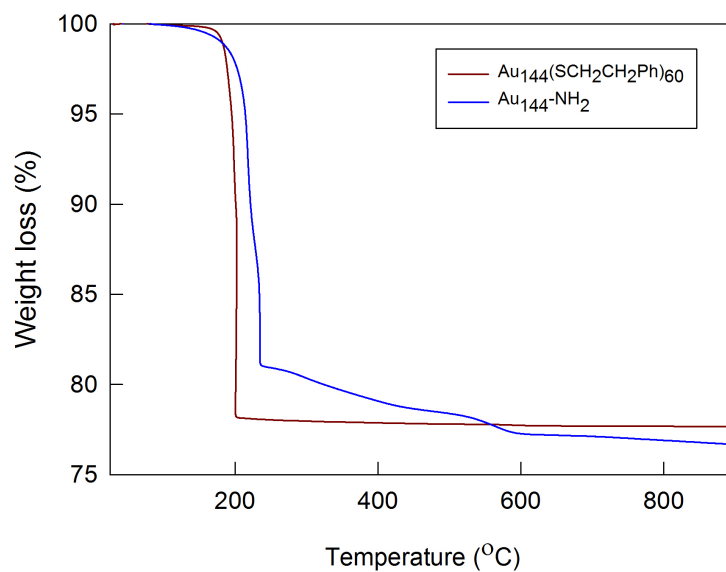


Figure S1. TGA of $\text{Au}_{144}(\text{SCH}_2\text{CH}_2\text{Ph})_{60}$ and $\text{Au}_{144}\text{-NH}_2$.

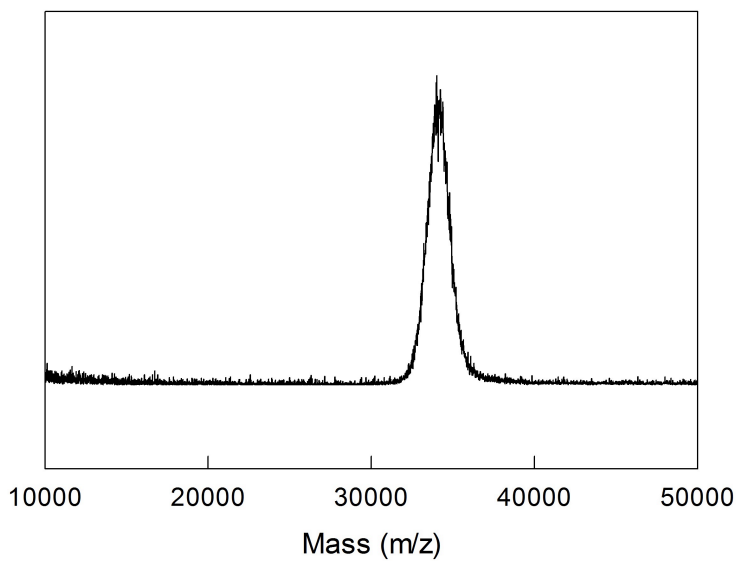


Figure S2. MALDI-TOF spectrum of $\text{Au}_{144}(\text{SCH}_2\text{CH}_2\text{Ph})_{60}$. The spectrum shows a maximum at 34.11 kDa, in agreement with previous observations of pure samples of the same cluster [S5,S6]. This value is lower than the theoretical mass of 36596.9 due to partial loss of ligands, as already observed and commented upon [S7]. The sharpness and symmetry of the peak indicate a very high purity of the sample.

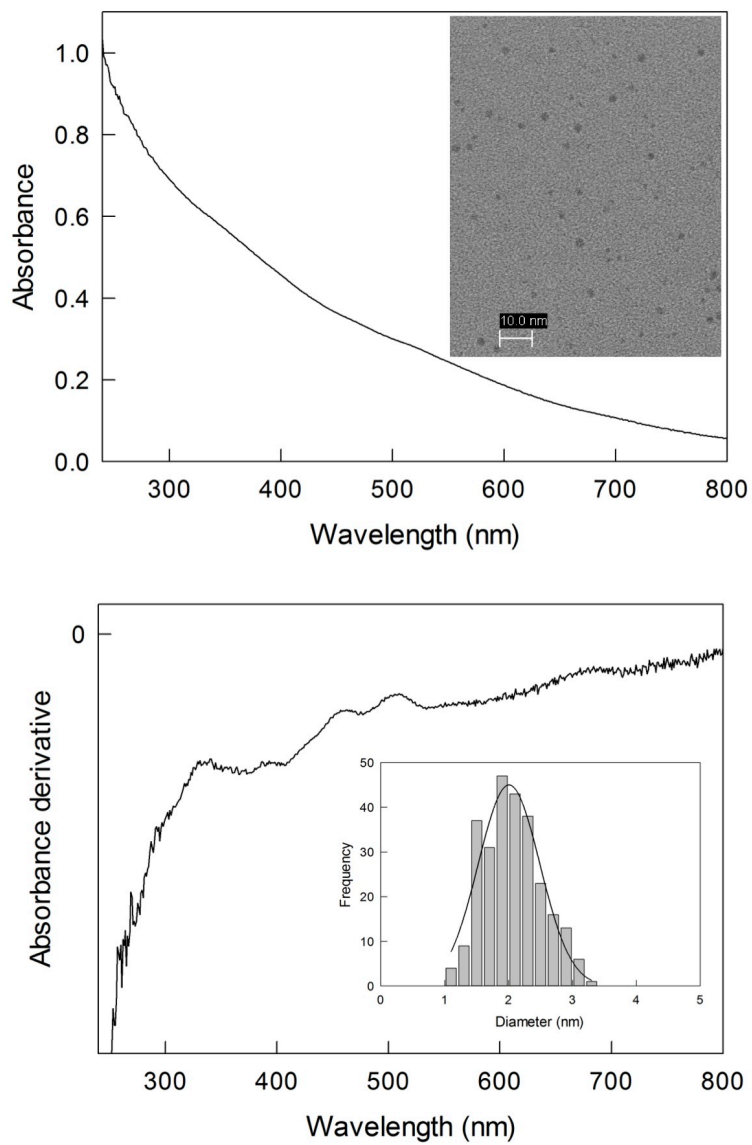


Figure S3. UV-vis absorbance and derivative spectra of $\text{Au}_{144}(\text{SCH}_2\text{CH}_2\text{Ph})_{60}$. Insets show an STEM image and the size distribution.

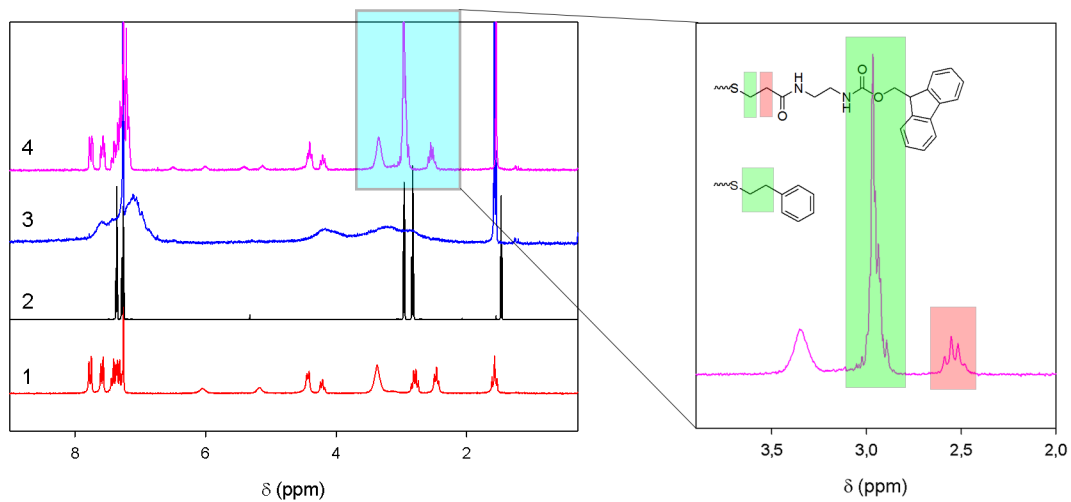


Figure S4. ¹H NMR spectra of (1) Fmoc-protected ligand **2**, (2) phenylethanethiol, (3) Au₁₄₄ MPC after ligand exchange reaction, and (4) the same gold nanocluster after decomposition with iodine. The inset highlights peak assignments. 200 and 400 MHz, CDCl₃, 23 °C.

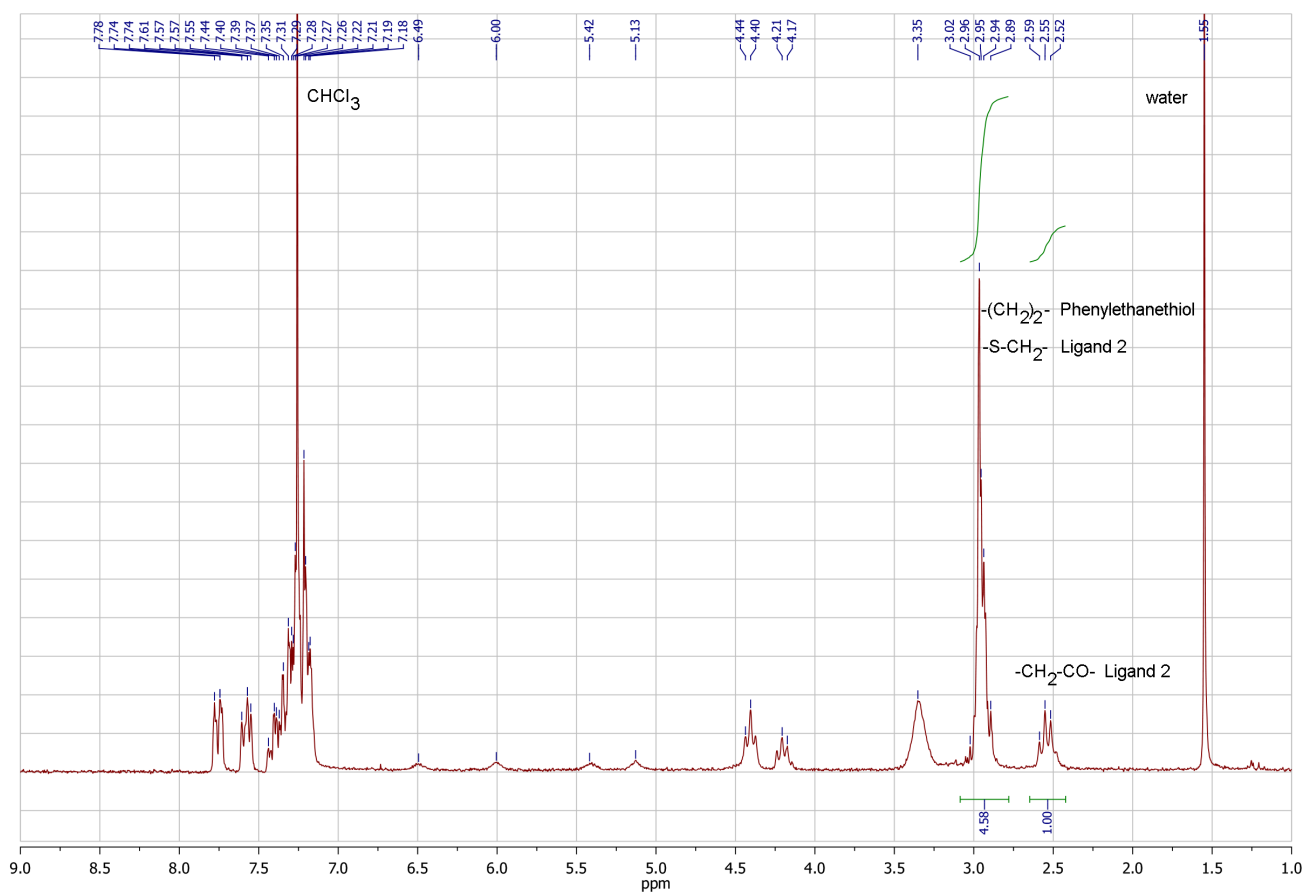


Figure S5. 200 MHz ¹H NMR spectra of Au₁₄₄(SCH₂CH₂Ph)₆₀ exchanged with 1 eq of ligand **2**, after decomposition with iodine. CDCl₃, 23 °C.

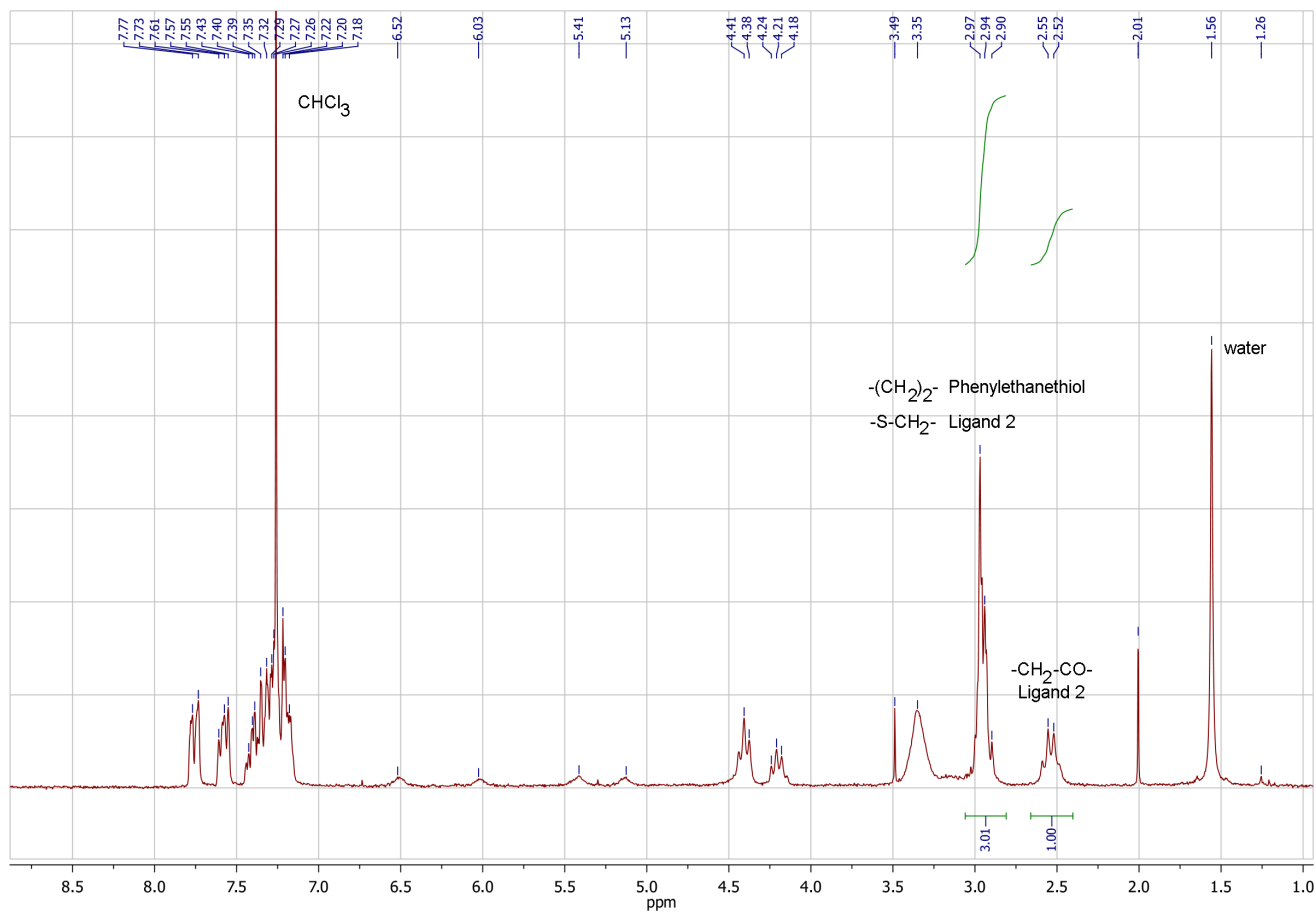


Figure S6. 200 MHz ^1H NMR spectra of $\text{Au}_{144}(\text{SCH}_2\text{CH}_2\text{Ph})_{60}$ exchanged with 1.5 eq of ligand **2**, after decomposition with iodine. CDCl_3 , 23 $^\circ\text{C}$.

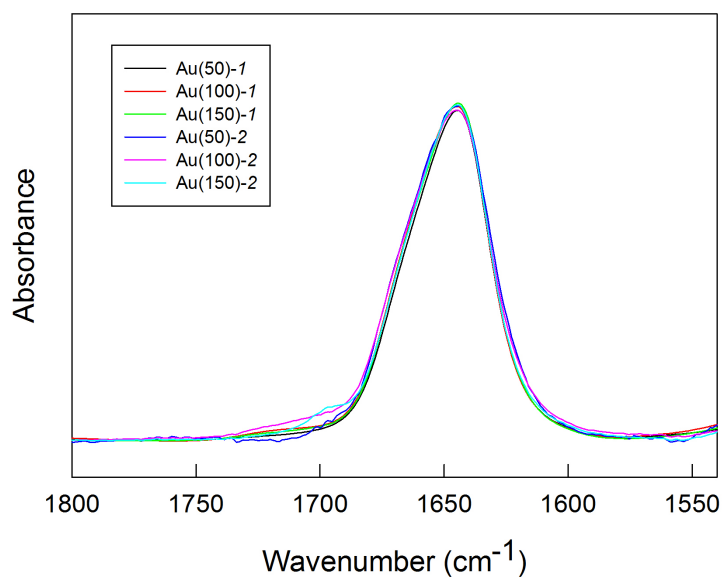


Figure S7. FT-IR spectra of the obtained core-shell nanoparticles in Amide I region (normalized to the absorbance of $\text{Au}(50)-1$).

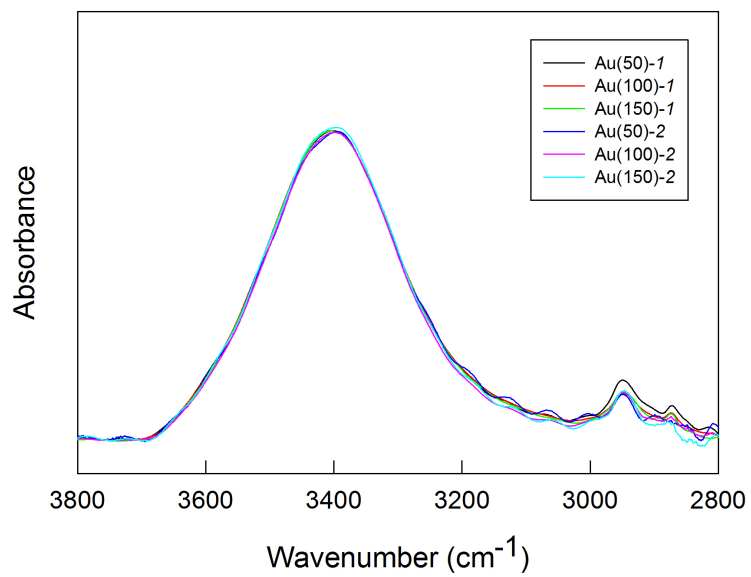


Figure S8. FT-IR spectra of the obtained core-shell nanoparticles in Amide A region (normalized to the absorbance of Au(50)-1).

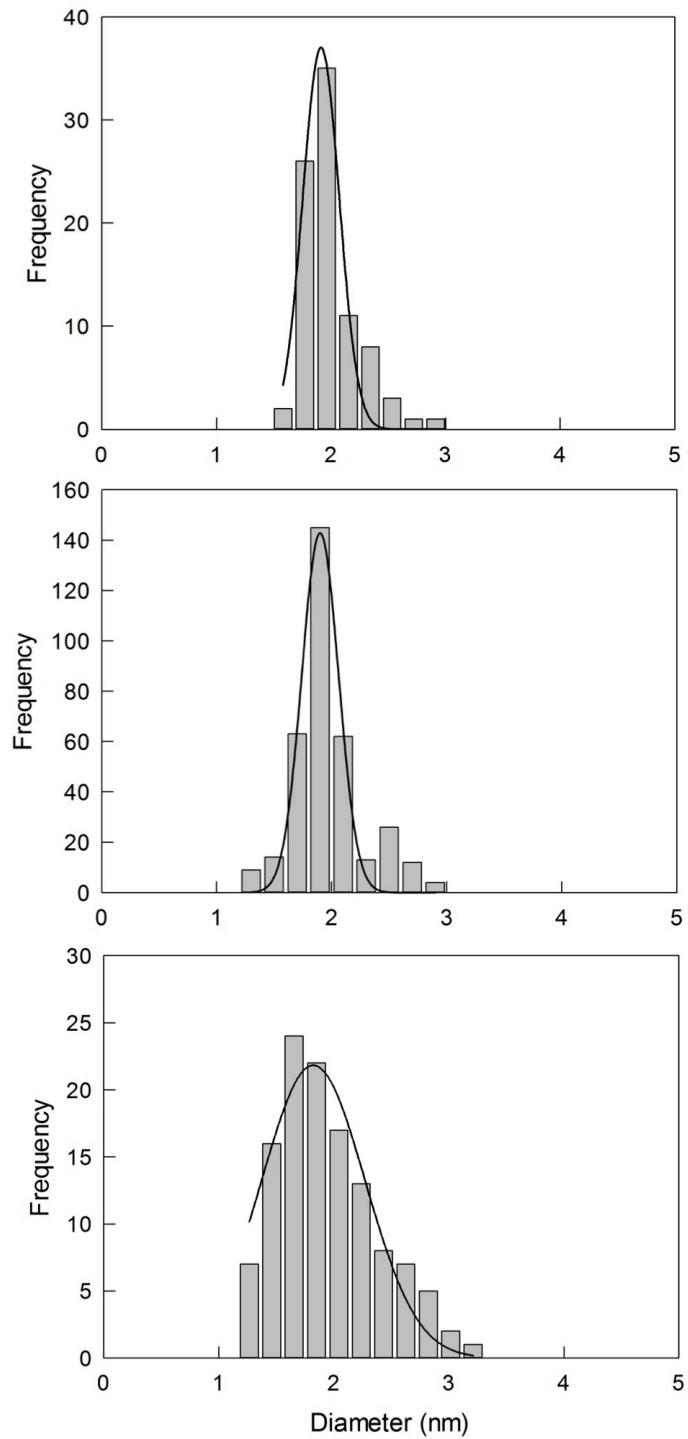


Figure S9. Size distribution in samples (top to bottom) Au(50)-I, Au(100)-I, and Au(150)-I.

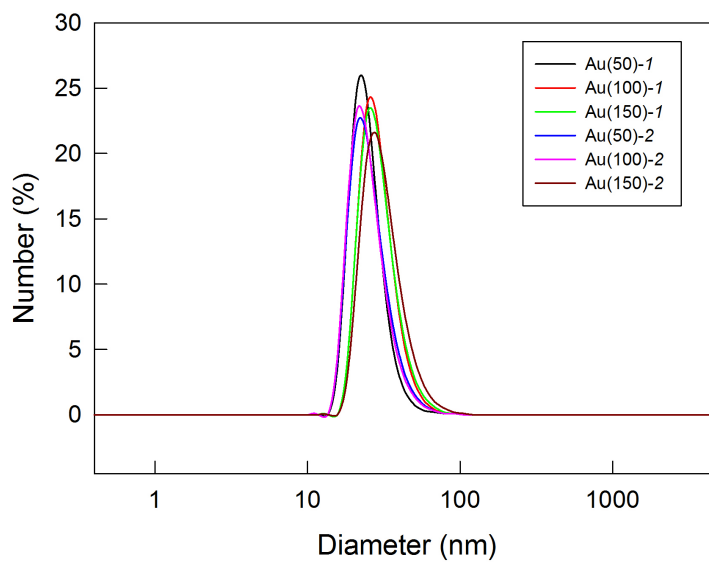


Figure S10. DLS spectra of core-shell nanoparticles (10 mg/ml in 1% HCl).

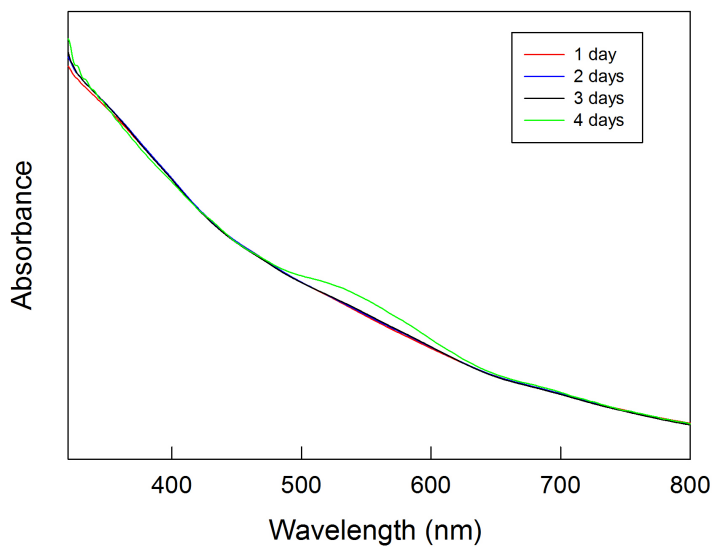


Figure S11. Time evolution of the optical absorption spectrum for Au(150)-1 during polymerization (CHCl₃).

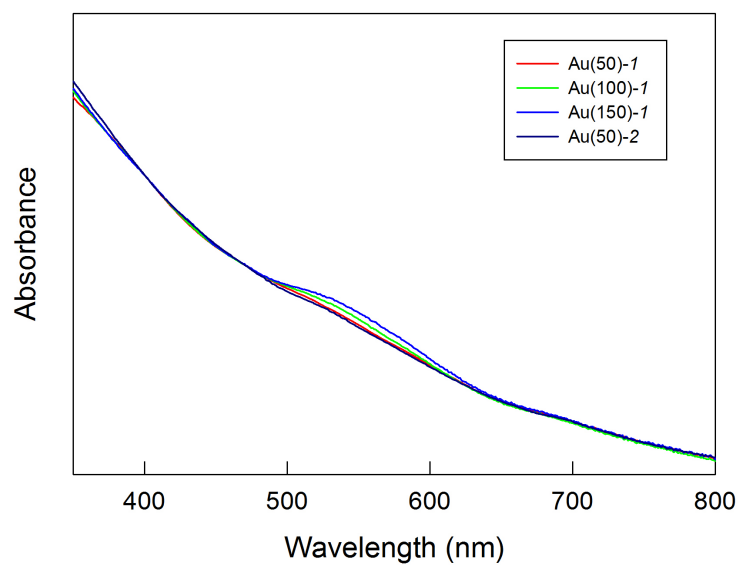


Figure S12. Comparison between UV-vis spectra of Fmoc-protected polylysine coated gold nanoclusters. The spectra of Au(100)-2 and Au(150)-2 are not shown because of their low solubility in CHCl_3 .

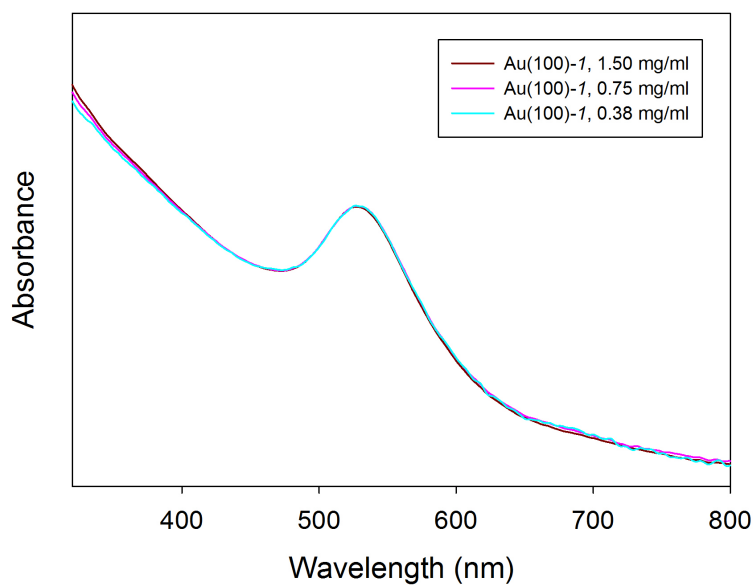


Figure S13. UV-vis spectra of the Au(100)-1 solution taken at different concentration after 1 day (normalized to lowest concentration).

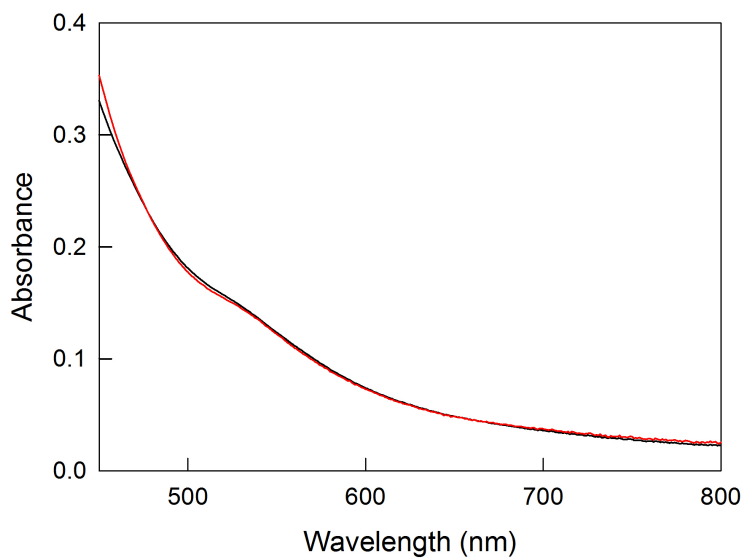


Figure S14. UV-vis spectra of Fmoc-protected and acetylated Au(100)-2 in DMF and 1% HCl/DMF, respectively. The spectra were taken after one week.

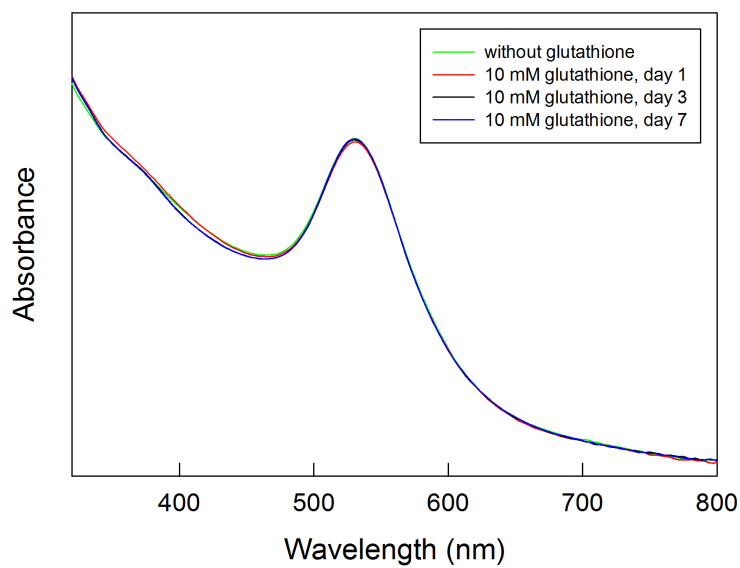


Figure S15. UV-vis spectra of Au(150)-1 in a 10 mM solution of glutathione.

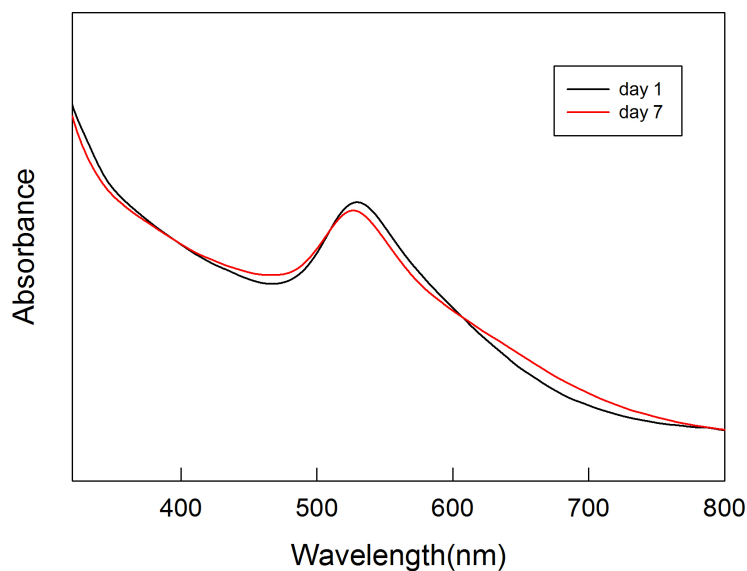


Figure S16. UV-vis spectra of Au(150)-1 in presence of a large amount of ethanethiol (300 equiv) with respect to the amount of initial phenylethanithiol ligands).

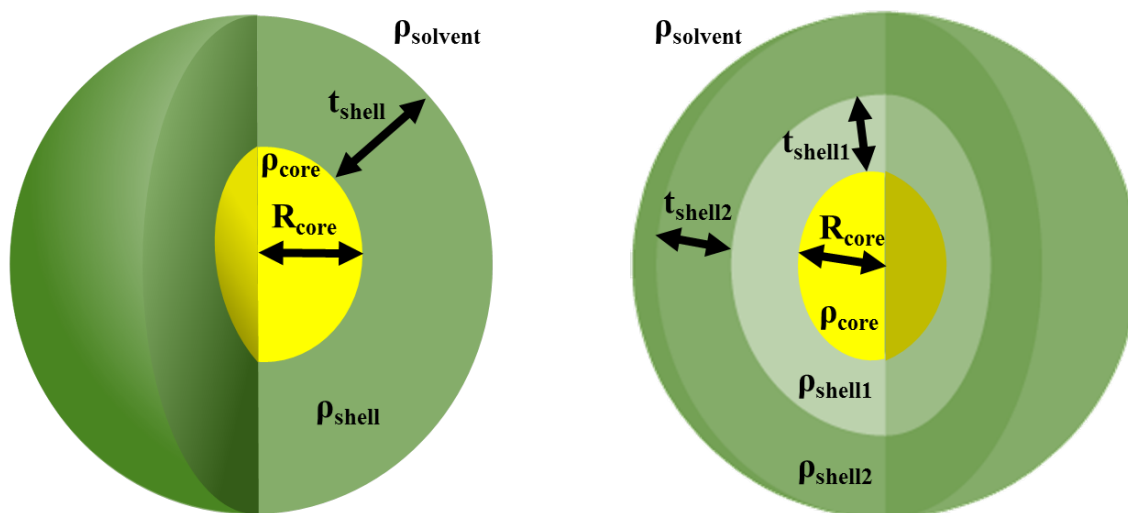


Figure S17. The sketches of core-single shell (left) and core-two shell (right) spherical model. The core and shell represent Au cluster and surface-attached ligands, respectively. ρ_x and t_x represents the electron density and shell thickness of part x , respectively. R_{core} represents the radius of the Au core.

5. References

- S1. A. H. Holm, M. Ceccato, R. L. Donkers, L. Fabris, G. Pace and F. Maran, *Langmuir*, 2006, **22**, 10584–10589.
- S2. L. Becucci, R. Guidelli, F. Polo and F. Maran, *Langmuir*, 2014, **30**, 8141–8151.
- S3. G. J. M. Habraken, M. Peeters, C. H. J. T. Dietz, C. E. Koning and A. Heise, *Polym. Chem.*, 2010, **1**, 514–524.
- S4. ftp://ftp.ncnr.nist.gov/pub/sans/kline/Download/SANS_Model_Docs_v4.10.pdf.

S5. H. Qian and R. Jin, *Nano Lett.*, 2009, **9**, 4083-4087.

S6. D. Bahena, N. Bhattarai, U. Santiago, A. Tlahuice, A. Ponce, S. B. H. Bach, B. Yoon, R. L. Whetten, U. Landman and M. Jose-Yacaman, *J. Phys. Chem. Lett.* 2013, **4**, 975-981.

S7. H. Qian and R. Jin, *Chem. Mater.* 2011, **23**, 2209-2217.